

## Response of the APV readout chip to laser-simulated, highly ionizing interactions

J. Bernardini, S. Gennai, R. Grabit, L. Mirabito

► **To cite this version:**

J. Bernardini, S. Gennai, R. Grabit, L. Mirabito. Response of the APV readout chip to laser-simulated, highly ionizing interactions. 2004. in2p3-00023377

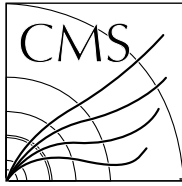
**HAL Id: in2p3-00023377**

**<http://hal.in2p3.fr/in2p3-00023377>**

Preprint submitted on 3 Dec 2004

**HAL** is a multi-disciplinary open access archive for the deposit and dissemination of scientific research documents, whether they are published or not. The documents may come from teaching and research institutions in France or abroad, or from public or private research centers.

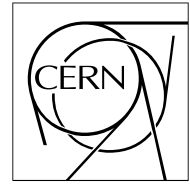
L'archive ouverte pluridisciplinaire **HAL**, est destinée au dépôt et à la diffusion de documents scientifiques de niveau recherche, publiés ou non, émanant des établissements d'enseignement et de recherche français ou étrangers, des laboratoires publics ou privés.



The Compact Muon Solenoid Experiment

# CMS Note

Mailing address: CMS CERN, CH-1211 GENEVA 23, Switzerland



7th October 2004

## Response of the APV readout chip to laser-simulated, highly ionizing interactions

J. Bernardini

*INFN Pisa Italy*

S. Gennai

*Scuola Normale Superiore Pisa, Italy*

R. Grabit, L. Mirabito<sup>a)</sup>

*CERN, Geneva, Switzerland*

### Abstract

Heavily Ionizing Particles are known to cause sizable dead-time in the front end APV [1] chip of the CMS Silicon Strip Tracker. To better understand this behavior, the effects of Highly Ionizing Particles in the CMS Silicon Strip Tracker were simulated using a 1060 nm laser. Calibrated laser pulses allow one to determine the energy threshold at which the dead-time becomes significant as well as the time evolution of the chip response. Various APV settings and supply line resistor values were investigated. Results agree with test beam data as well as previous laboratory measurements in confirming that settings can be found for which the dead-time is as low as 100ns for up to 50 MeV deposited energy.

---

<sup>a)</sup> Also Institut de Physique Nucleaire de Lyon, France

# 1 Introduction

In October 2001, six CMS silicon detector modules were operated in the CERN X5 beam line [2] where they were exposed to 120 GeV/c pions. The data included a few anomalous events in which the readout front-end electronics was in saturation following a large release of energy in the micro-strip sensor. These events were typically characterized by a very high positive signal on the small number of strips actually collecting the charge released while all other channels connected to the same APV readout chip are brought down well below pedestal values and beyond the lower endpoint of the dynamic range. This saturation persists for several hundred nanoseconds during which all channels of the chip are inefficient. This behavior was traced to the feedback on the branch feeding the APV inverter stage to which all channels are connected. During normal operation this feedback loop acts to minimize any common mode noise. The effect was reproduced in laboratory tests [2] where its temporal structure was also studied. In particular it was noticed that during recovery, the APV baseline can overshoot its nominal working point for several hundred nanoseconds.

The high energy releases in the micro-strip sensors can be explained by the occurrence of inelastic interactions in the detector material, accompanied by the creation of showers and highly ionizing debris. These events are referred to as "Highly Ionizing Particles" (HIP). A dedicated test [3] using 300 MeV/c pions was performed at the Paul Scherrer Institute (PSI) in April 2002. The low energy pion beam reproduced the mean interaction rate that the CMS tracker will experience in LHC operation [4] and thus made it possible to measure the rate of occurrence of HIP events in a "CMS-Like" environment.

To further investigate the impact on chip operation, measurements of the chip recovery time with various APV settings were performed with a dedicated laser setup. In this case the high energy release associated with a HIP event is obtained by means of a calibrated laser pulse. A second laser pulse then produces a signal equivalent to a Minimum Ionizing Particle (MIP) after a variable delay time to test the extent to which the detector efficiency has recovered from the simulated HIP event. The induced inefficiency as a function of delay time could thereby be studied as a function of the deposited HIP energy and the value of the resistance used in the inverter stage. These measurements are complementary to the results obtained from beam tests and other laboratory studies to assess the effect of HIP events on the CMS Silicon Strip Tracker [2, 3, 5].

In the remainder of this paper we describe our laboratory setup and then examine how the APV chip baseline recovers following a HIP event. Finally we present our measurements of the subsequent dead-time incurred by the chip in response to these events.

## 2 Laboratory Setup

### 2.1 Readout Modules

Measurements were made using one of the Tracker Outer Barrel (TOB) detector modules previously deployed in the pion beam test at PSI. This module has two 500  $\mu\text{m}$  thick Si sensors and 4 APV chips. It was originally equipped with a 100  $\Omega$  inverter resistor. The latter was changed to 50  $\Omega$  in response to previous HIP event studies that showed this value improves the chip's response.

The two APV chip working modes were investigated: "peak" mode (low occupancy) where each pre-amplifier is readout at the peak voltage of the CR-RC shape signal, and "deconvolution" mode for high luminosity running where an analog weighted sum of 3 samples (-25 ns, 0 ns, +25 ns) is performed suppressing the rising and falling tail of the pulse.

The front-end hybrid handling the APV chips was connected via an electrical adaptor board in an identical manner to that used for both the X5 and PSI beam tests. A detailed description of the front-end readout system can be found in [6]. Readout control consists of one Front-End Controller PMC board connected to one Control Chip Unit (CCU). The CCU propagates the 40 MHz clock and trigger signals to the hybrid. It also provides the I2C bus line to the hybrid in order to control the various front-end chips.

The analog readout is done electrically from the hybrid to the 40 MHz flash ADC (Front End Driver prototype in PMC form factor). The trigger system consists of a Trigger Sequence Card [7] externally triggered by the pulser triggering the MIP signal from the laser.

A single PC runs the front-end control and data acquisition via a standalone [8] program. This program is able to run the various calibration tasks needed to commission the Si detector, i.e. pedestal, timing alignment, pulse shape on calibration pulse or signal, etc. It acquires and stores data in a way that's compatible with the standard tracker data acquisition used in beam tests [9]. Finally it can be used to perform a full charge cluster analysis of the data using the same algorithms used for the PSI beam test.

## 2.2 Laser Setup

The setup consists of two 1060 nm lasers triggered by a narrow ( $< 3$  ns) pulse in order to get well-calibrated pulse lengths during laser relaxation. The two lasers were positioned over strips on the second sensor of the TOB module that are readout by the same APV chip but separated by roughly 100 channels (approximately 2 cm). With the help of a spherical lens at the end of each laser fiber, the light from each laser was focused on only one strip, just beyond the surface metal. The intensity of one laser was then increased to produce a charge deposition comparable to a HIP event while the second was calibrated to produce a MIP pulse. The data acquisition was synchronized with the latter. The MIP pulse was subsequently delayed relative to that of the HIP in order to study the MIP detection efficiency as a function of time after the occurrence of the HIP signal. Figure 1 shows event snapshots for 11 different runs taken for one particular setup of the system. The first snapshot corresponds to the module prior to HIP injection while the following 10 correspond to the module at delay times relative to the HIP signal starting with a 100 ns delay and increasing in increments of 100 ns. For this particular setup it is seen that the HIP signal completely screens any MIP signal occurring less than 600 ns later.

## 2.3 HIP calibration

The charge deposited by the HIP pulse was evaluated using the bias current of the Si module. The level of the ever-present dark current increases as a result of the charge injected by the HIP. If the pulse rate  $R$  is sufficiently high, the increase  $\Delta I$  can be measured with a nano-ammeter [10]. The energy  $E_{HIP}$  is then obtained as:

$$E_{HIP} = \frac{\Delta I}{e R E_{pair}}$$

where  $e$  is the electron charge, and  $E_{pair} = 3.6$  eV is the energy required to extract an electron-hole pair in Si. For comparison, the energy released by a MIP in traversing  $500 \mu\text{m}$  of Si is roughly 140 keV, corresponding to 39000 e-hole pairs.

The stability of the charge collection and thus that of the measurement, was verified over a broad range of injection rates as shown in figure 2. The limited precision of the current measurement limited the HIP energies we were able to scan to values above  $\sim 10$  MeV.

The HIP pulse intensity is controlled by two parameters: the laser bias voltage and the width of the light pulse. We fixed the width and performed a scan of the bias voltage. The linear dependence of the intensity up to a maximum HIP energy of 50 MeV is shown in figure 3.

During calibration of the laser it was discovered that the module was not perfectly shielded from light. This leads to a 10 % systematic uncertainty in the measurement of the bias current and hence also in the HIP intensity.

### 3 APV recovery measurement

The recovery of the APV after a HIP event is studied in this section in terms of the recovery of the signal baseline and MIP signal efficiency.

#### 3.1 Baseline and signal recovery

A baseline shift normally reflects an increase in the common mode level seen by the chip. This common mode level is evaluated as the truncated mean, i.e. without the 10 % highest and 10 % lowest charged strips out of the 128 channels of the APV. Pedestals are subtracted after the common mode level is determined.

In the present study we restricted the calculation to blocks of 32 strips in order to obtain a clearer signal without fake clusters resulting from baseline distortions due to the HIP. For the plots shown below, the common mode level was estimated using blocks of 32 strips that do not contain either of the strips targeted by laser for the HIP and MIP signals. This differs from the beam test measurements in the sense that both the baseline shift and the signal measurements are less affected by the occurrence of the HIP.

The laser cluster signal is reconstructed by associating strips with signal to noise greater than 3 to a peak signal strip with signal to noise greater than 5. In all of the comparisons below, the signal over noise is normalized to that of the MIP laser when no HIP is fired.

Figure 4 shows the mean common mode level on the APV and MIP signal size as a function of time after the HIP signal is fired using data collected in "peak" mode for a TOB module equipped with a 100  $\Omega$  inverter resistor. It shows also the signal recovery.

To further study signal recovery without requiring the strip thresholds generally used in the cluster formation algorithm, we take advantage of the known MIP laser position and follow the time evolution of the central signal strip charge (after subtraction of the raw data pedestal and common mode level). Similarly, a non-hit strip after subtraction of raw pedestals is used to follow baseline evolution. Figures 5,6, and 7 show the subsequent behavior of the APV for various modes of operation: Peak mode with inverter stage off, and Deconvolution mode with inverter stage on or off.

From these studies one notes the following:

- For HIP events which have energies below 20 MeV, the signal recovery starts as soon as the baseline reenters the dynamic range, while for HIP energies higher than 20 MeV the signal recovery is delayed relative to the baseline recovery.
- The recovery is fastest in peak mode.
- Turning off the inverter stage causes the baseline to saturate at the positive end of the dynamic range, as expected. It then quickly oscillates and may saturate for a long time in the opposite polarity.

Dead time is defined as the amount of time for which there is no sensitivity to the MIP signal. The effective inefficiency thus depends also on the signal to noise ratio required for inclusion of strips in signal clusters. We require a signal to noise greater than 3<sup>1)</sup>. For non-irradiated modules the mean signal to noise ratio is 23 while after radiation roughly 50 % of this is lost due to increased noise. It follows that full efficiency is recovered in an irradiated module once 25 % of signal is recovered. Table 1 summarizes the results in standard conditions (deconvolution mode, inverter stage on) for dead time and full efficiency recovery time with various HIP energies.

---

<sup>1)</sup> The previous cut of  $\frac{S}{N} > 5$  can be relaxed to 3 to obtain higher efficiency without significantly increasing the noise occupancy.

HIP energies (MeV)	Dead Time (ns)	Full efficiency recovery time (ns)
15	100	200
25	500	800
35	600	700
45	700	800

Table 1: Measured dead times and recovery times for full efficiency (25 % of signal recovery) in standard operating conditions for various HIP energies using a 100  $\Omega$  inverter resistor

Comparing these results with those obtained in previous laboratory tests [2], we find qualitatively similar behavior but a much stronger dependence on HIP energy. In the previous study the Si sensor was simulated by a capacitive network so that charge was directly injected into 1 or 2 APV channels. In our study, the signal was injected into a single Si sensor strip but neighboring strips show a huge signal also. The average number of saturated strips in our study is 4, which is comparable to the number seen in test beam. The difference in number of saturated strips may explain the discrepancies in the two laboratory studies. It is however confirmed that the dead time becomes insignificant for HIP energies approaching 10 MeV.

Additionally, it is noticed that turning off the inverter stage induces equivalent inefficiencies for very high energy depositions but improves recovery times for lower energy depositions. Thus for example, no inefficiency is observed up to 25 MeV.

### 3.2 Comparison between 50 $\Omega$ and 100 $\Omega$ inverter resistors

Previous measurements [2, 3] suggest that the dead time due to a HIP event should be reduced by decreasing the value of the inverter stage resistor. The same TOB module as discussed above was used with the inverter resistor changed from 100  $\Omega$  to 50  $\Omega$ . Figures 8,9,10, and 11 show the corresponding baseline and signal recovery for this case. Two main changes are seen:

- When the inverter stage is on, the baseline recovery is faster and the signal recovery now follows that of the baseline, leading to a notable reduction in the full efficiency recovery time as summarized in Table 2.
- If the inverter is off, the baseline oscillation is reduced and the full efficiency dead time is maintained below 100 ns in all cases. Baseline saturation and inefficiency is observed only at the 50 ns delay point relative to the HIP occurrence. Full efficiency is observed at all other delay points.

HIP energies (MeV)	Dead Time (ns)	Full efficiency recovery time (ns)
15	100	100
23	150	150
28	250	250
31	300	300

Table 2: Measured dead times and recovery times for full efficiency (25 % of signal recovery) in standard operating conditions for various HIP energies using a 50  $\Omega$  inverter resistor.

## 4 Summary

Highly Ionizing Particles are produced by nuclear interactions in Si tracking sensors. They are observed to produce large signals that can saturate APV readout chips for some time. Detailed studies of this effect have been made using a laser setup at CERN. In particular, the dependence of the dead time on the

resistor used in the supply line of the APV inverter stage is measured. These studies qualitatively confirm the findings of previous measurements that better performance is obtained, either with the inverter stage on or off, when a 50  $\Omega$  inverter resistor is used. In this case the dead time for full efficiency is maintained below 100 ns even for very large energy depositions.

Further measurements using the final front end ADC for which pedestal and common mode level computations are performed by FPGA chips are expected to confirm that this dead time can be kept to a negligible level.

## Acknowledgments

We would like to thank Alan Honma for his help in modifying modules and Joe Incandela for his precious reading and correction of this work.

## References

- [1] “The APV25 deep sub micron readout chip for CMS channels detectors”, L.Jones et al, Proceedings of 5th workshop on Chips electronics for LHC experiments, CERN/LHCC/99-09, 162-166
- [2] “The effect of Highly Ionising Events on the APV readout chips”, R.Bainbridge et al., CMS Note 2002/038
- [3] “Test beam analysis of the effect of Highly Ionising Particles on Silicon strip Tracker”, W.Adam et al, CMS Note 2003/025
- [4] “Highly Ionising events in Silicon detectors”, M. Huhtinen, CMS Note 2002-011
- [5] “Laboratory studies of the HIP and pin-hole effects on the APV”, M.Raymond, [http://cmsdoc.cern.ch/~ghall/TKEL\\_0102/Raymond\\_0102.pdf](http://cmsdoc.cern.ch/~ghall/TKEL_0102/Raymond_0102.pdf)
- [6] “The Tracker project technical design report”, CERN/LHC 98/6
- [7] “The Trigger Sequencer Card user’s manual”, M.Ageron et al., <http://l3info.in2p3.fr/cms/tsc/tsc03.pdf>
- [8] “The tracker data acquisition user’s guide”, L. Mirabito, CMS IN 2004/019
- [9] “Tracker data acquisition for beamtest and integration”, L.Mirabito et al., CMS IN 2003/021
- [10] “Result of radiation hardness of a Small Gap Chamber”, D.Bouvet et al., NIM A545, 359-363, 2000.

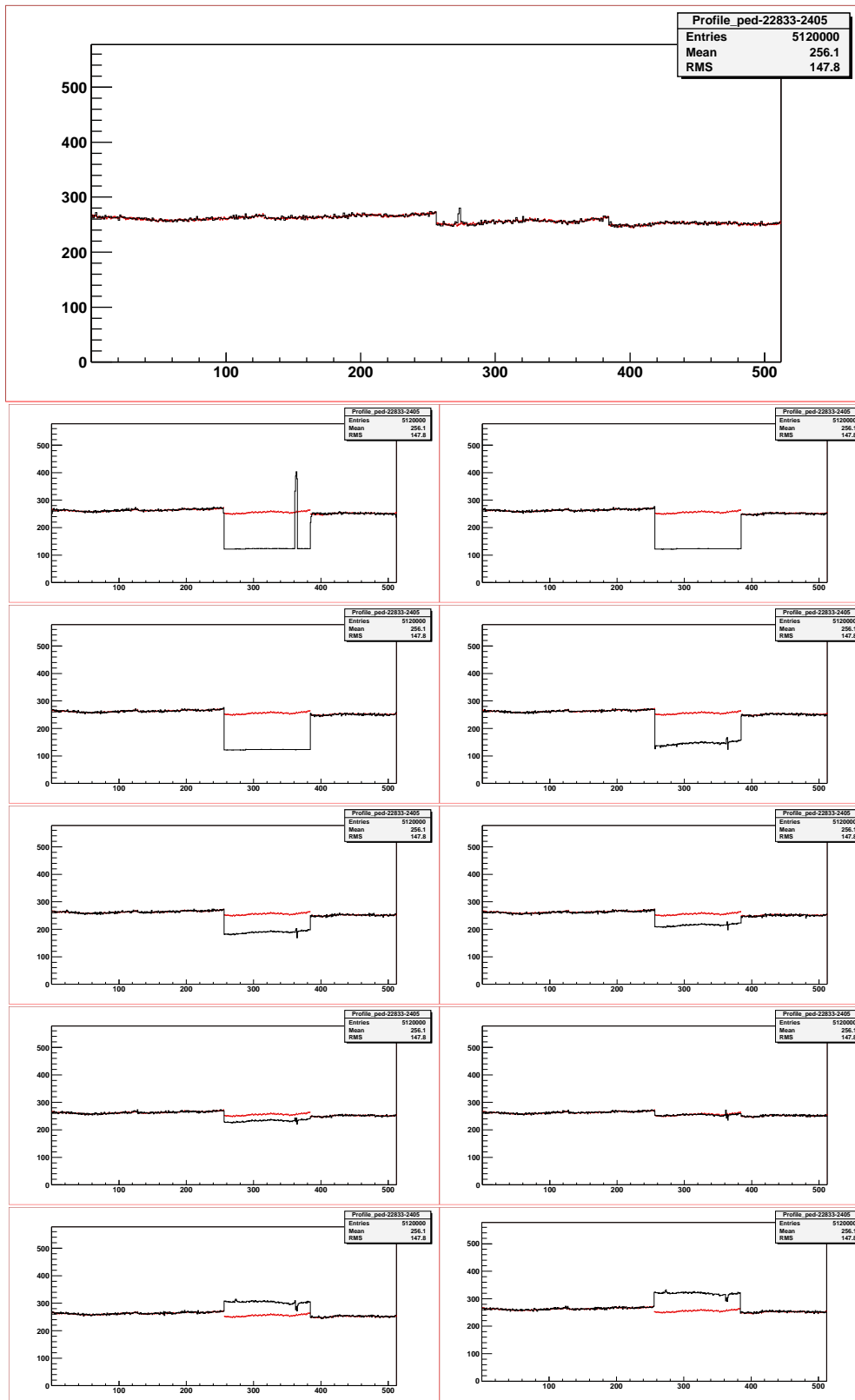


Figure 1: Raw events after laser HIP and MIP injections. The plots show raw ADC count (0 to 600) versus detector strip number (1 to 512). The first plot is an event with no HIP injection. The other 10 plots show events after HIP injection and MIP injection with the latter occurring with delays ranging from 0 to 900 ns in 100 ns steps. The baseline does not recover for  $\sim 600$  ns, screening the MIP signal completely.



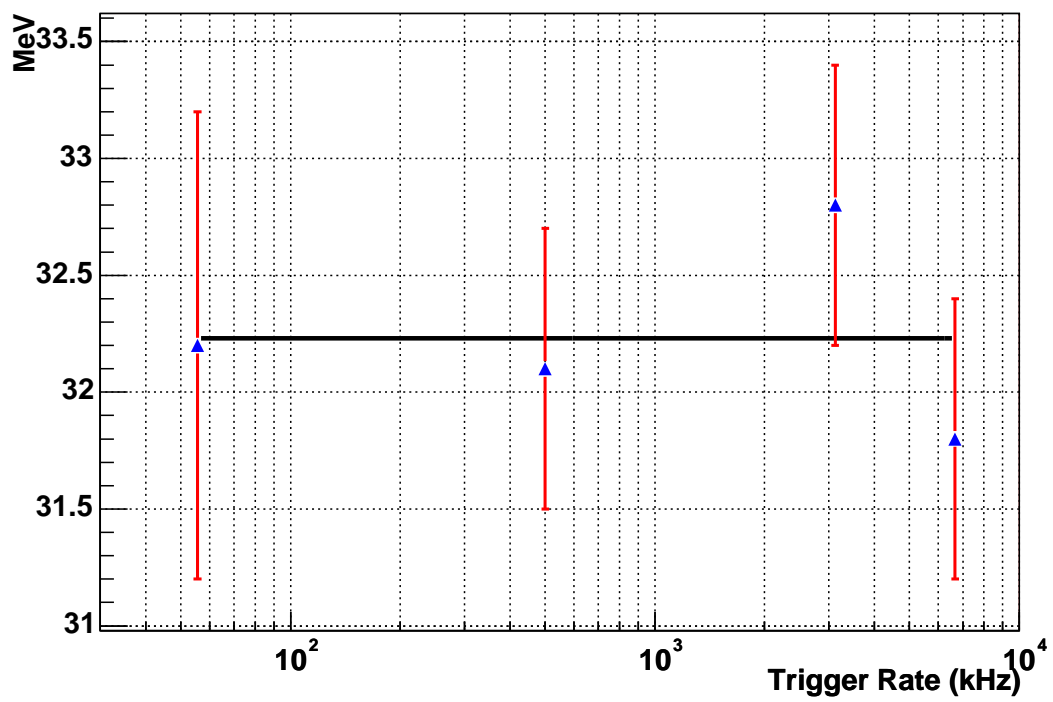


Figure 2: HIP energy measurement deduced from the current versus the injection rate.

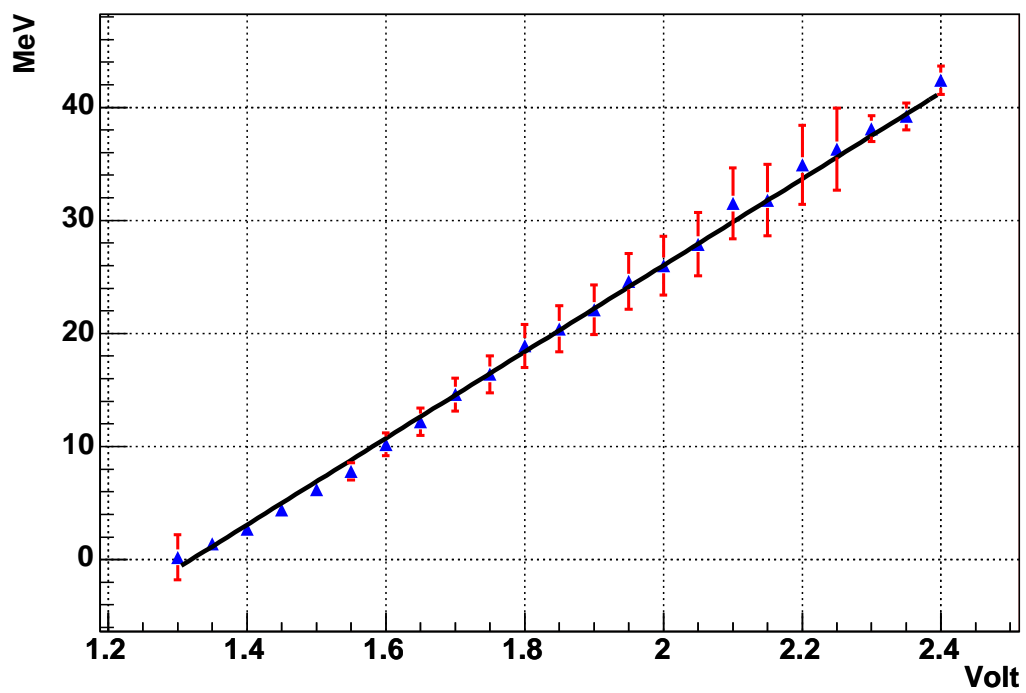


Figure 3: Laser bias voltage calibration curve for an integration time of 5.5 ns

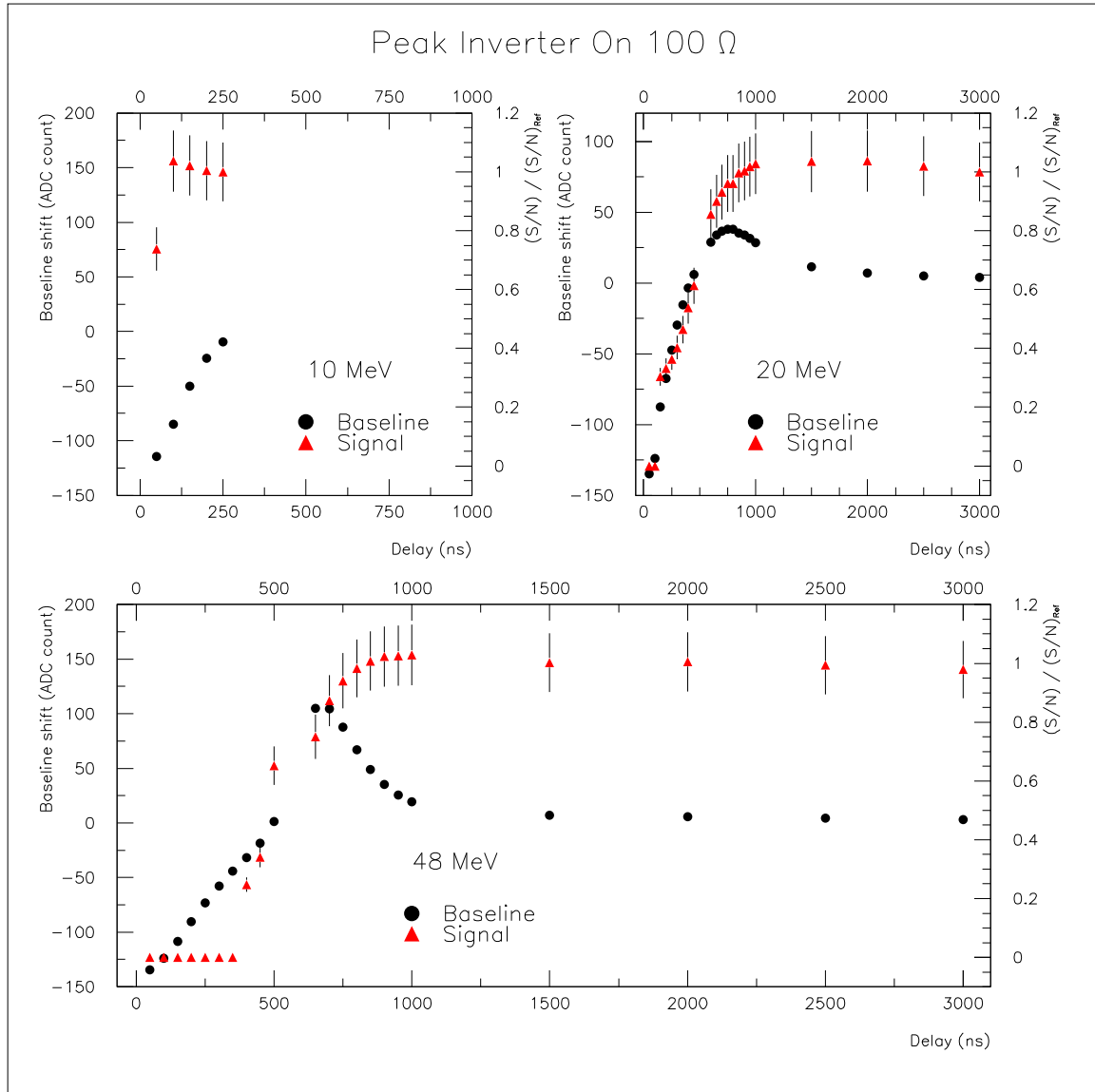


Figure 4: Time evolution of the computed common mode level (black dots), expressed in terms of ADC counts of the APV chip operating in peak mode for a TOB module with 100  $\Omega$  inverter resistor. The cluster signal evolution (red triangle) is also shown. Different HIP amplitudes are considered. The signal over noise is normalized to the measured one without HIP injection.

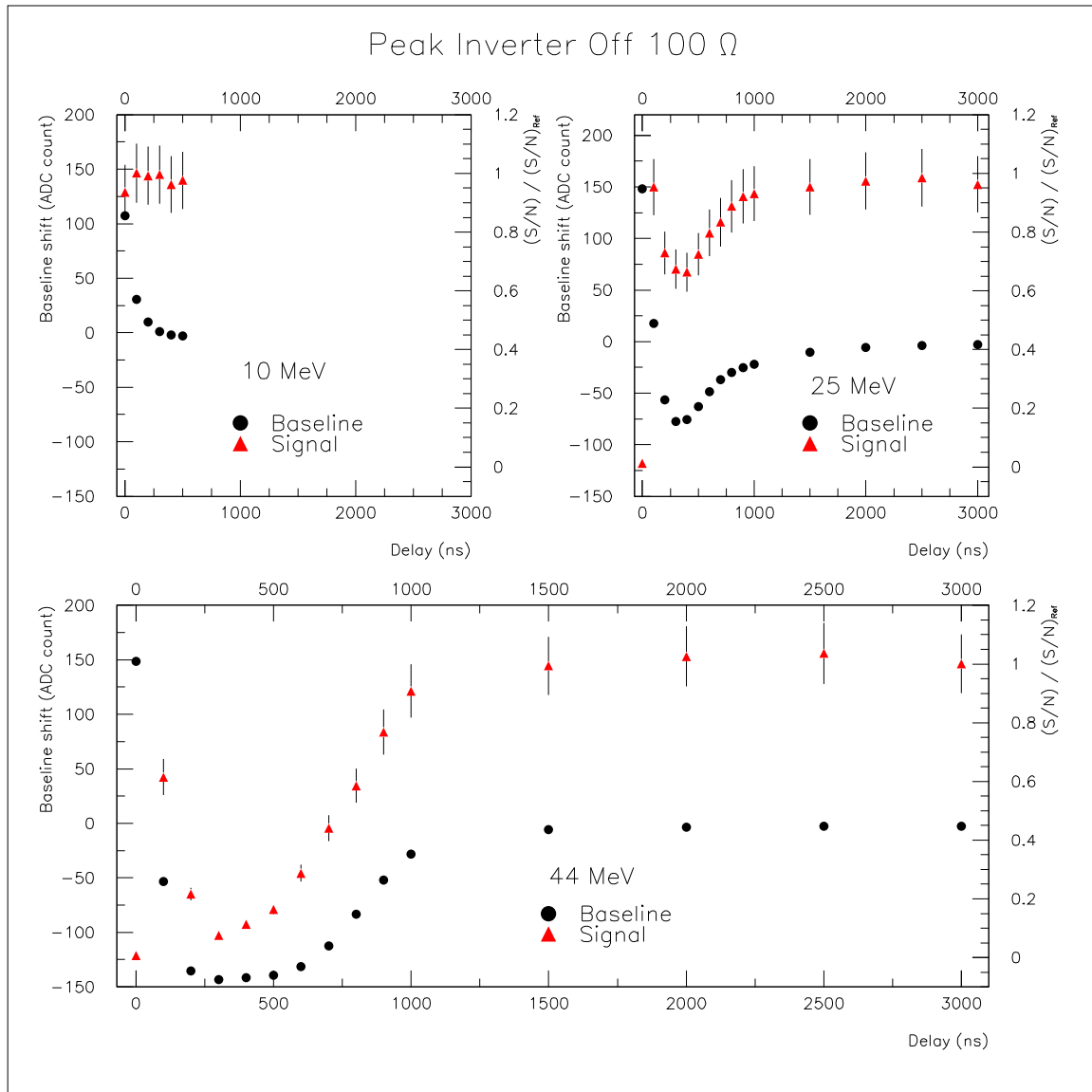


Figure 5: Baseline and signal recovery in Peak mode with inverter stage turned off for different HIP amplitudes. Black dots represents baseline shift, red triangles represent signal over noise normalized to the case of no HIP injection.

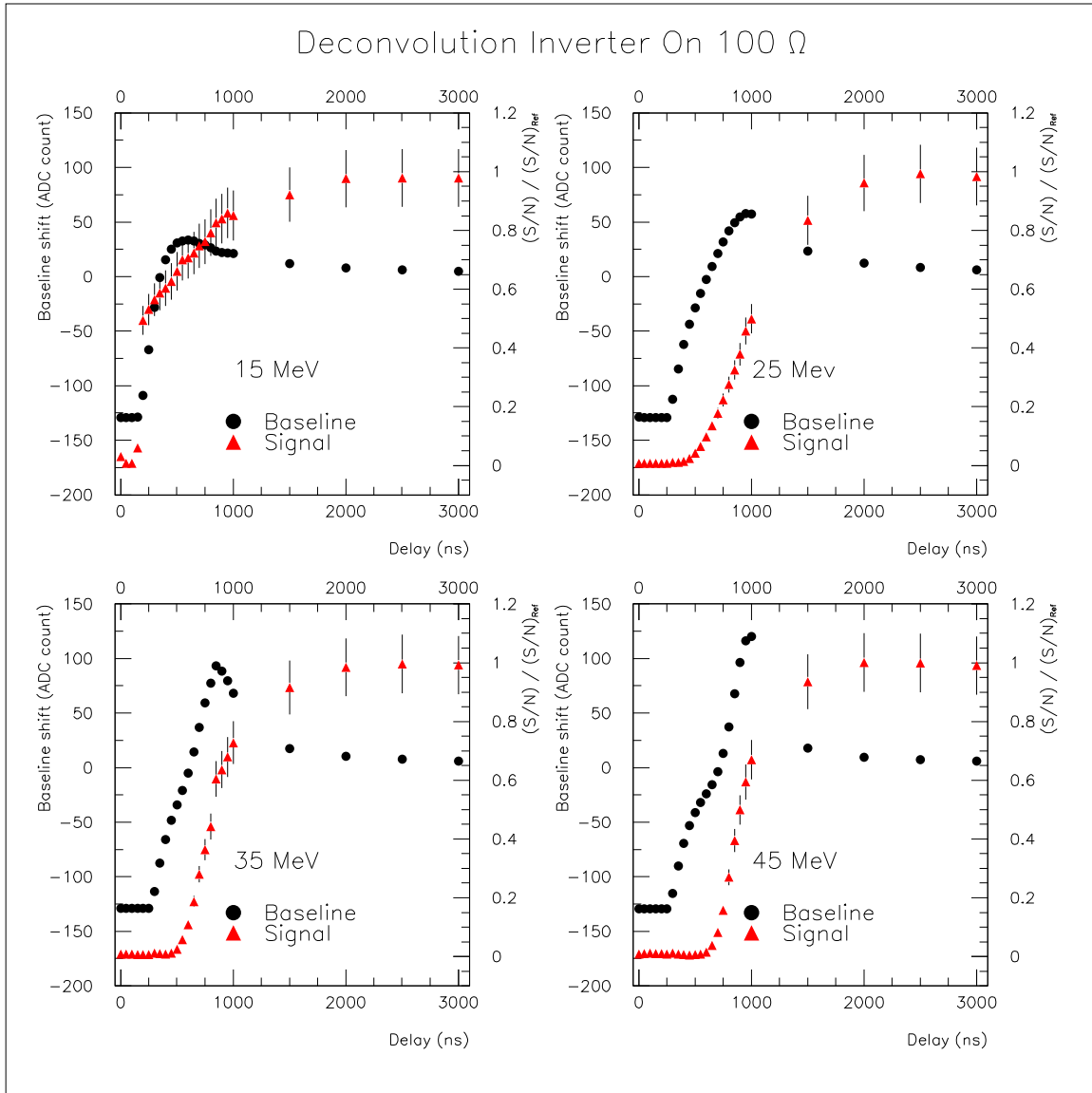


Figure 6: Baseline and signal recovery in Deconvolution mode with inverter stage turned on for different HIP amplitudes. Black dots represents baseline shift, red triangles represent signal over noise normalized to the case of no HIP injection.

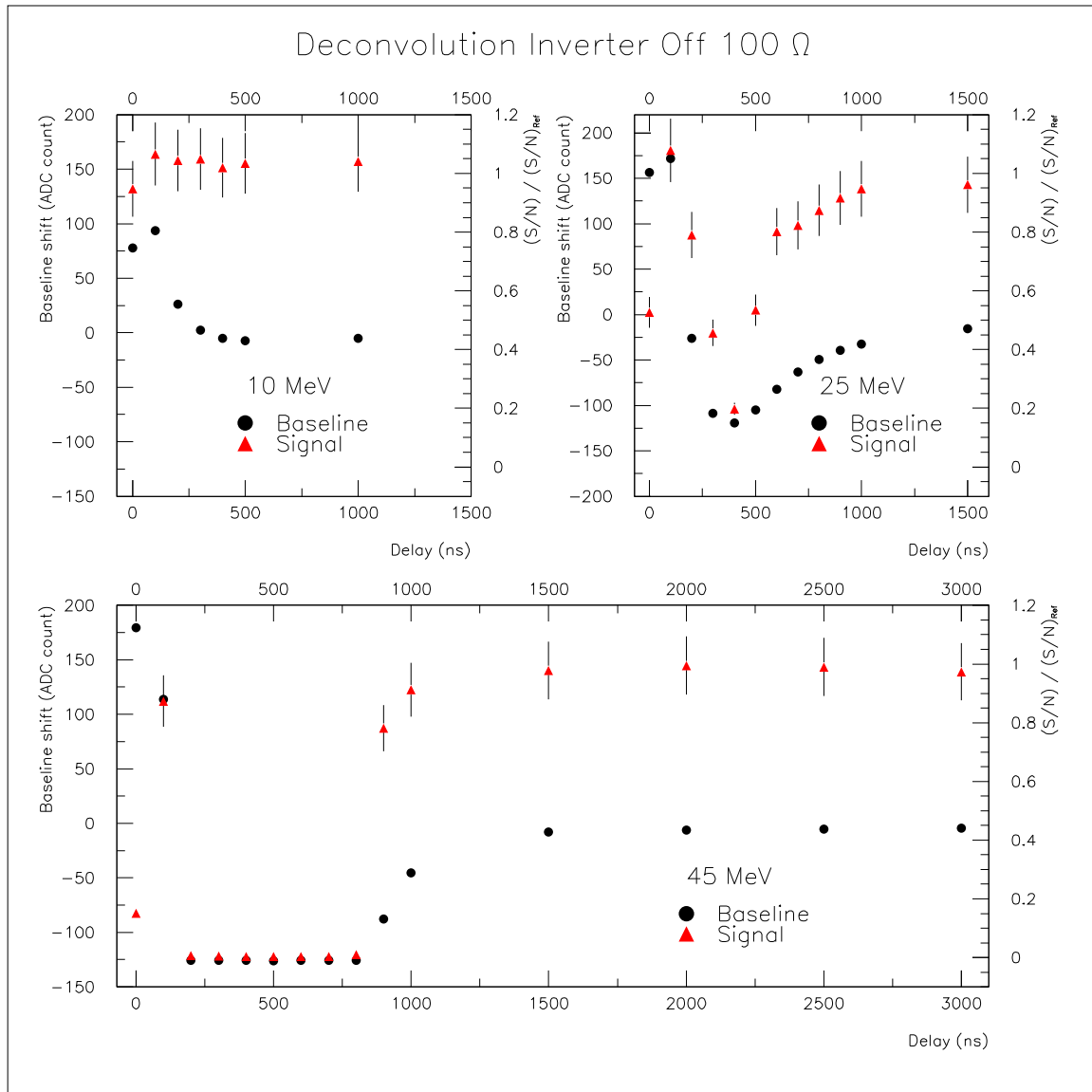


Figure 7: Baseline and signal recovery in Deconvolution mode with inverter stage turned off for different HIP amplitudes. Black dots represents baseline shift, red triangles represent signal over noise normalized to the case of no HIP injection.

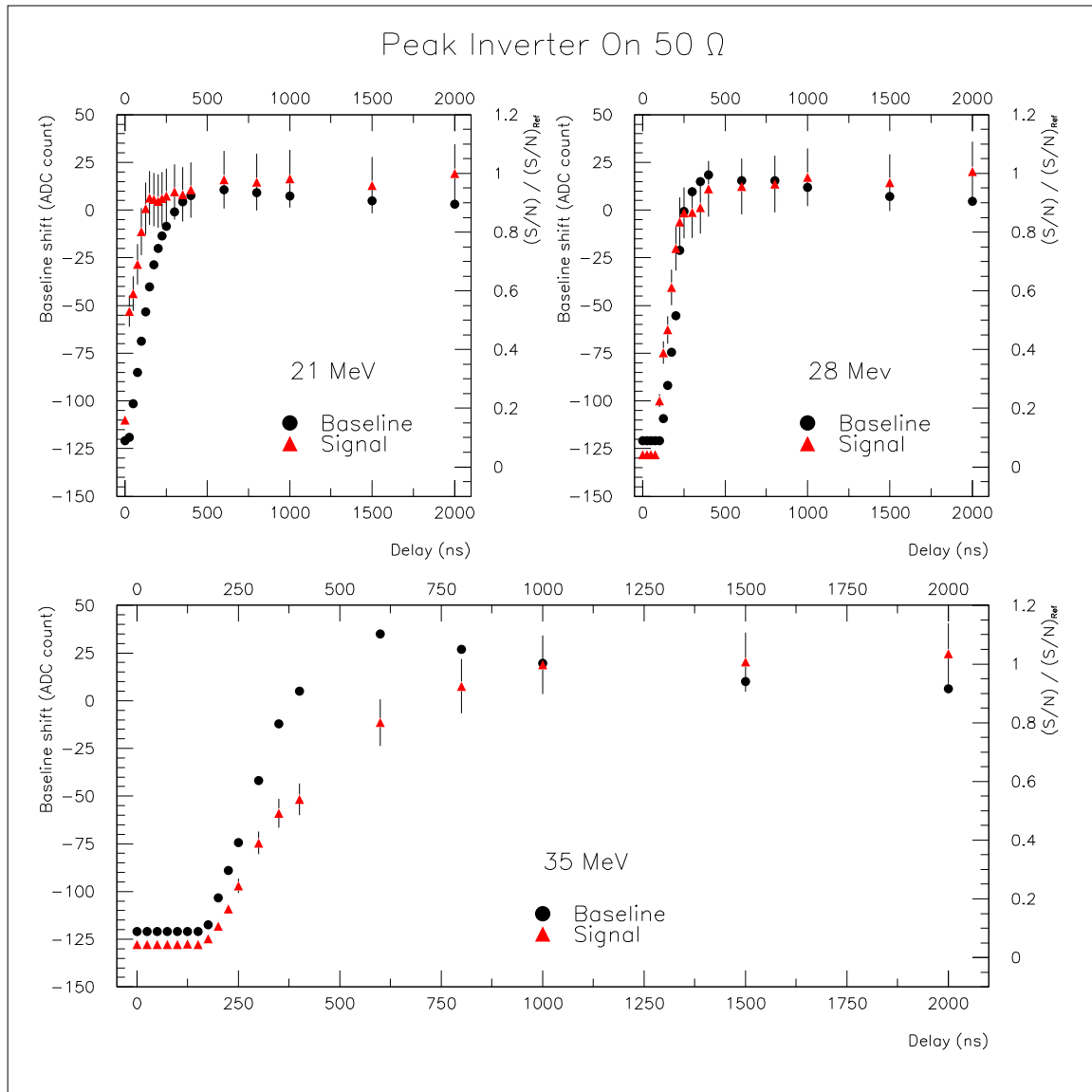


Figure 8: Baseline and signal recovery in Peak mode with inverter stage turned on for different HIP amplitudes and  $50 \Omega$  resistor . Black dots represents baseline shift, red triangles represent signal over noise normalized to the case of no HIP injection.

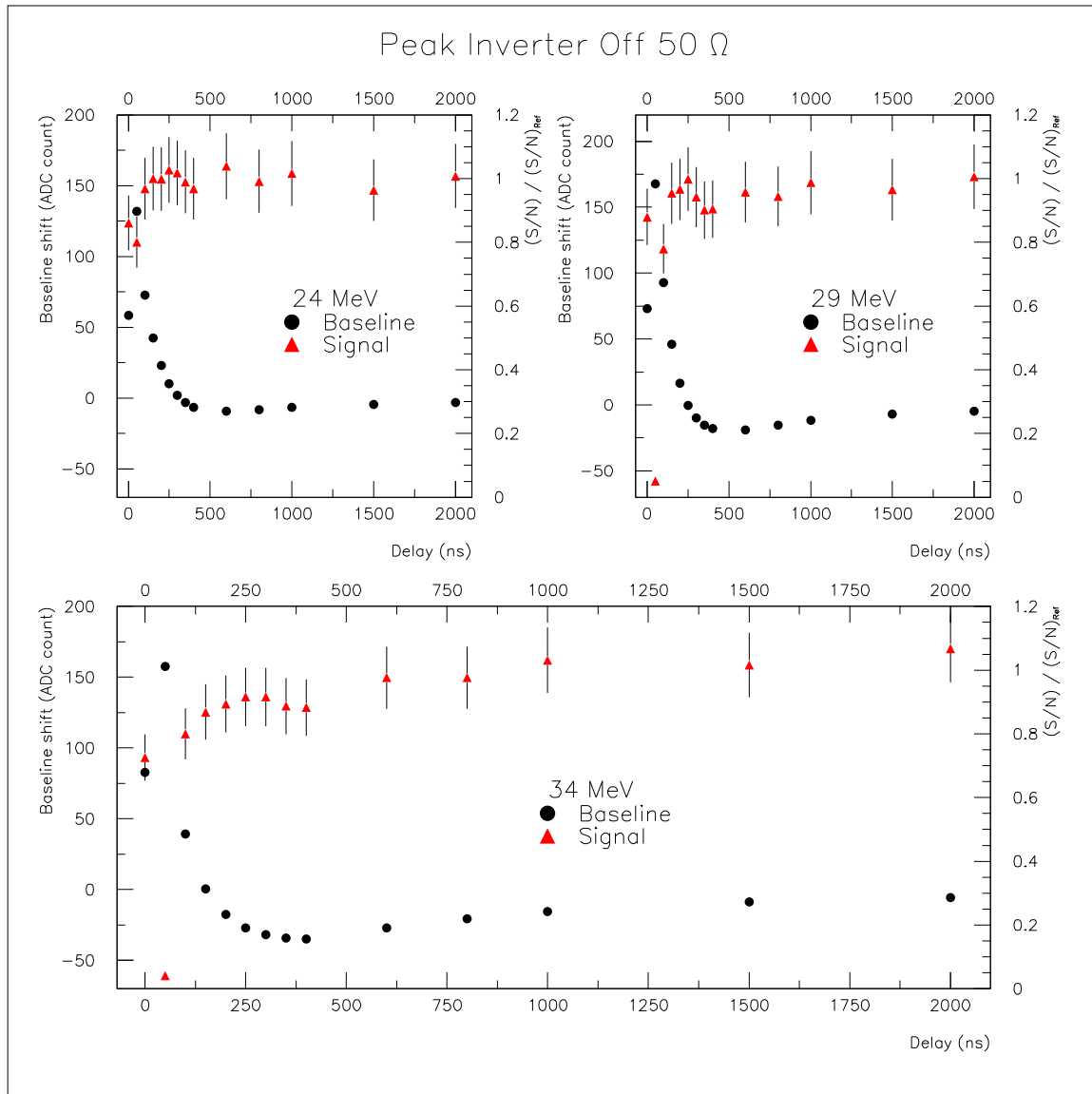


Figure 9: Baseline and signal recovery in Peak mode with inverter stage turned off for different HIP amplitudes and  $50 \Omega$  resistor. Black dots represents baseline shift, red triangles represent signal over noise normalized to the case of no HIP injection.

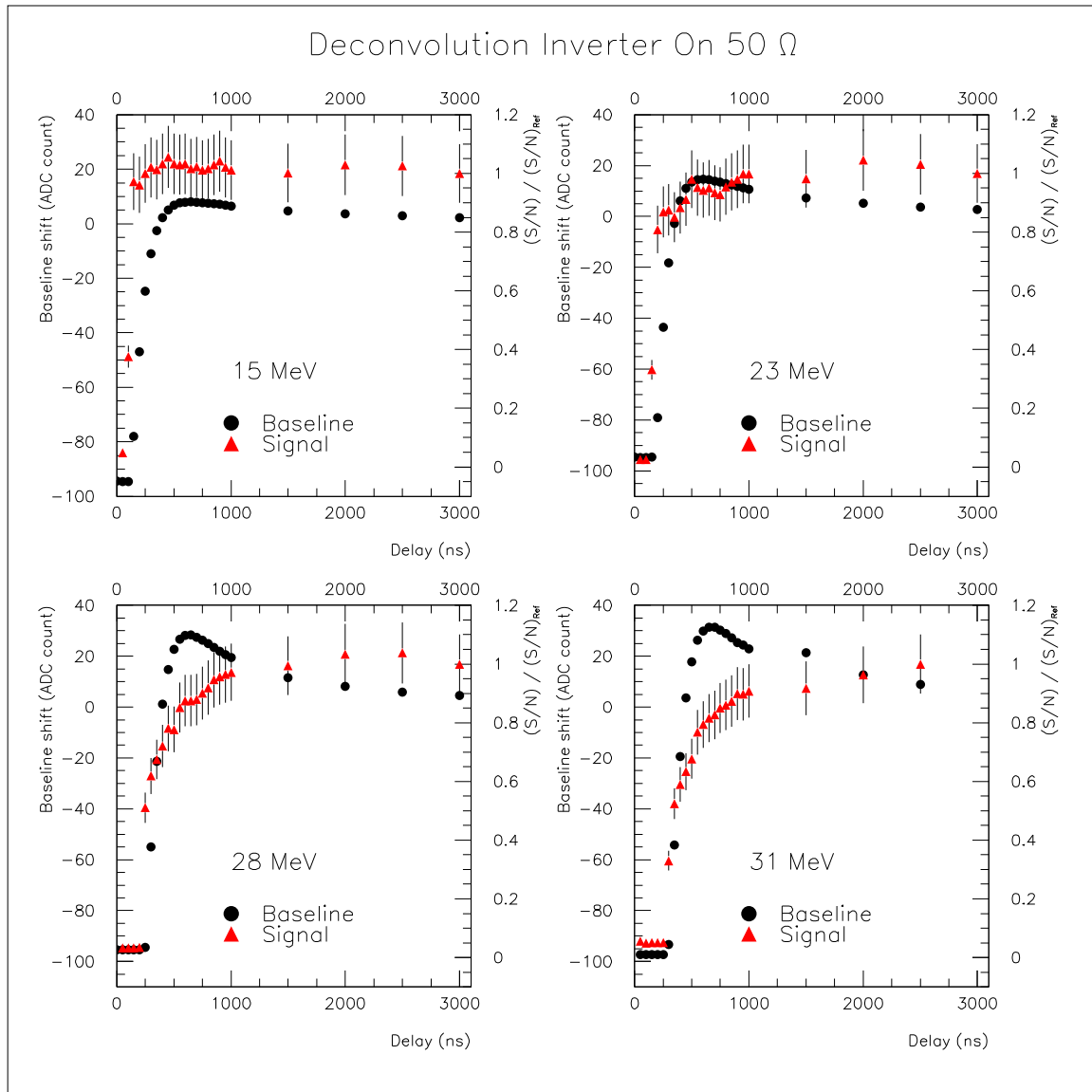


Figure 10: Baseline and signal recovery in deconvolution mode with inverter stage turned on for different HIP amplitudes and 50  $\Omega$  resistor. Black dots represents baseline shift, red triangles signal over noise recovery. The signal over noise is normalized to the measured one without HIP injection.



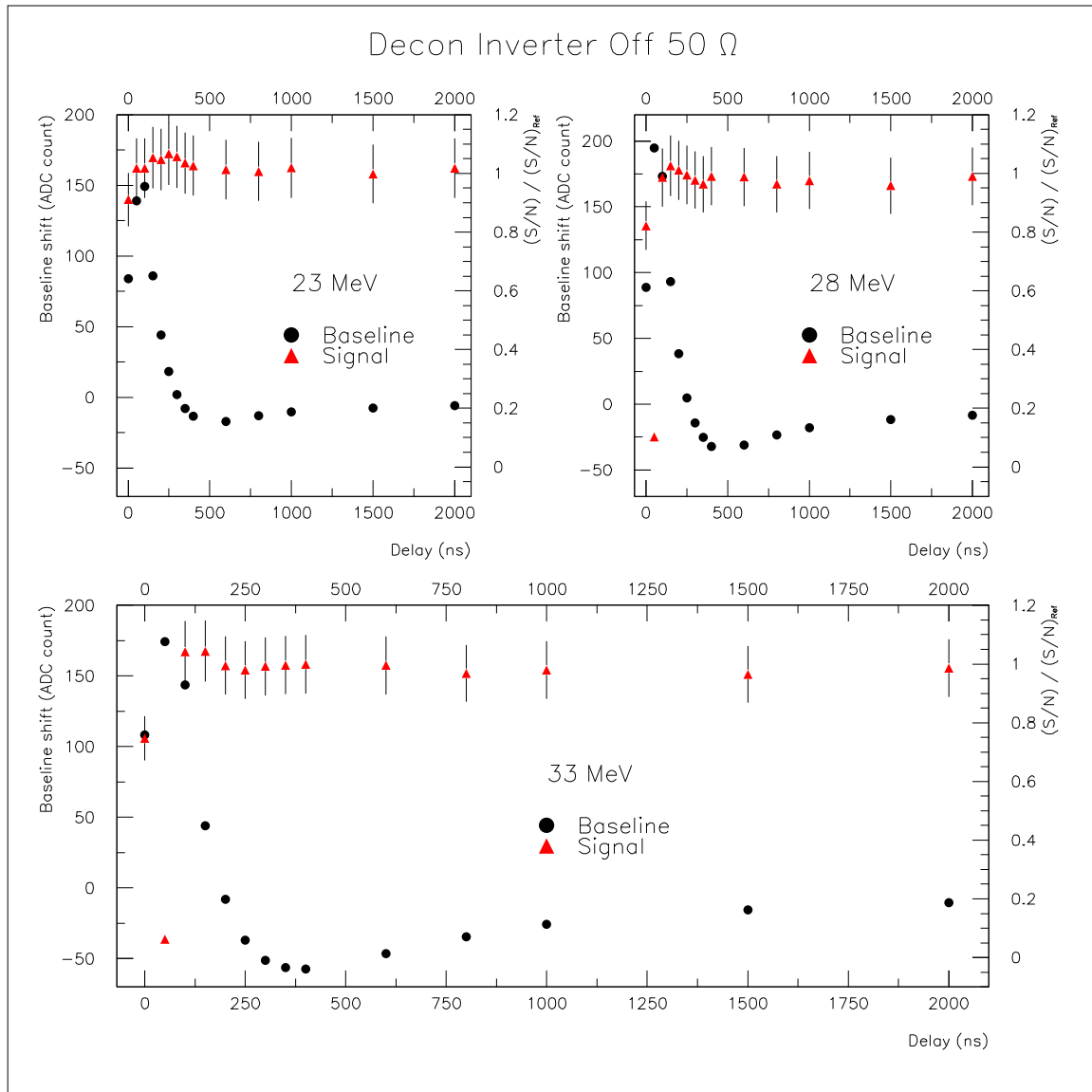


Figure 11: Baseline and signal recovery in deconvolution mode with inverter stage turned off for different HIP amplitudes and  $50 \Omega$  resistor. Black dots represent baseline shift, red triangles represent signal over noise normalized to the case of no HIP injection.